Phosphate vibrations probe local electric fields and hydration in biomolecules

Nicholas M. Levinson,[†] Erin E. Bolte,[‡] Carrie M. Miller,[‡] Steven Corcelli[‡,*] and Steven G. Boxer[†,*]

[†] *Department of Chemistry, Stanford University, Stanford, California, 94305 and* [‡] *Department of Chemistry and Biochemistry, University of Notre Dame, Notre Dame, Indiana 46556*

Supporting Information

Vibrational Stark Spectra

Phospholipid/solvent samples were loaded into sample cells comprised of CaF_2 windows (Red Optronics) coated with a 4 nm layer of Ni metal and separated by 26 μm plastic spacers. The sample cells were connected to the end of a stark rod designed to facilitate the attachment of electrodes to the coated CaF_2 windows, and the samples were flash frozen by plunging them into a purpose-built liquid nitrogen immersion cryostat. A high voltage power supply was used to apply a large DC voltage (~3500V for 1.4MV/cm electric fields) across the sample cell. Spectra were recorded at 1 cm^{-1} resolution using a vertex 80 FTIR (Bruker Optics), synchronized to the high voltage power supply. Stark spectra are the difference between the field on and field off absorbance spectra, which were determined from 128 scans with the applied field on and 128 scans with the applied field off. All Stark spectra scaled with the square of the applied field, as expected for isotropic samples.

Sample preparation

We screened several phospholipid/solvent combinations in order to identify an experimental system in which the phosphate bands in the IR spectra were clearly resolved from features arising from other vibrations of the phospholipid and solvent. All phospholipids were phosphoethanolamines, and differed only in the nature of the fatty acid chains, which are unlikely to affect the Stark properties of the phosphate group. In the infrared spectra of 250 mM 1-palmitoyl-2-oleoyl-*sn*-glycero-3-phosphoethanolamine (POPE) in glass forming solvents the absorption band corresponding to the symmetric stretch of the phosphate was clearly resolved, but the band corresponding to the antisymmetric stretch was obscured by a series of overlapping peaks due to CH_2 wagging vibrations of the palmitoyl fatty acid chains (Figure S1A, upper panel)[1]. Despite the complexity of the absorbance spectrum, the Stark spectrum of this sample (Figure S1A, lower panel) is dominated by a single feature arising from the PO_2^- antisymmetric stretch, indicating that the Stark effect for this stretch is unusually large. Since the CH_2 wagging bands arise from saturated fatty acid chains we reasoned that reducing the degree of saturation of the phospholipid fatty acid chains would improve the spectra. As expected, the overlapping CH_2 wagging bands were less prominent in absorbance spectra of 250 mM 1,2-dioleoyl-*sn*-glycero-3-phosphoethanolamine (DOPE) in toluene (Figure S1B), and not apparent in spectra of 1,2-didocosahexaenoyl-*sn*-glycero-3-phosphoethanolamine

(DDHEPE) in toluene (Figure S1D). The DDHEPE samples therefore provided the best spectra for determining the linear Stark tuning rate for the antisymmetric stretch of the phosphate. Deuterated toluene was used to shift a solvent peak that overlaps with the absorption band of the phosphate symmetric stretch (Figure S1B,C). The large Stark effect observed around 1150 cm^{-1} most likely arises from the stretching mode of the ester carbon-oxygen bonds.

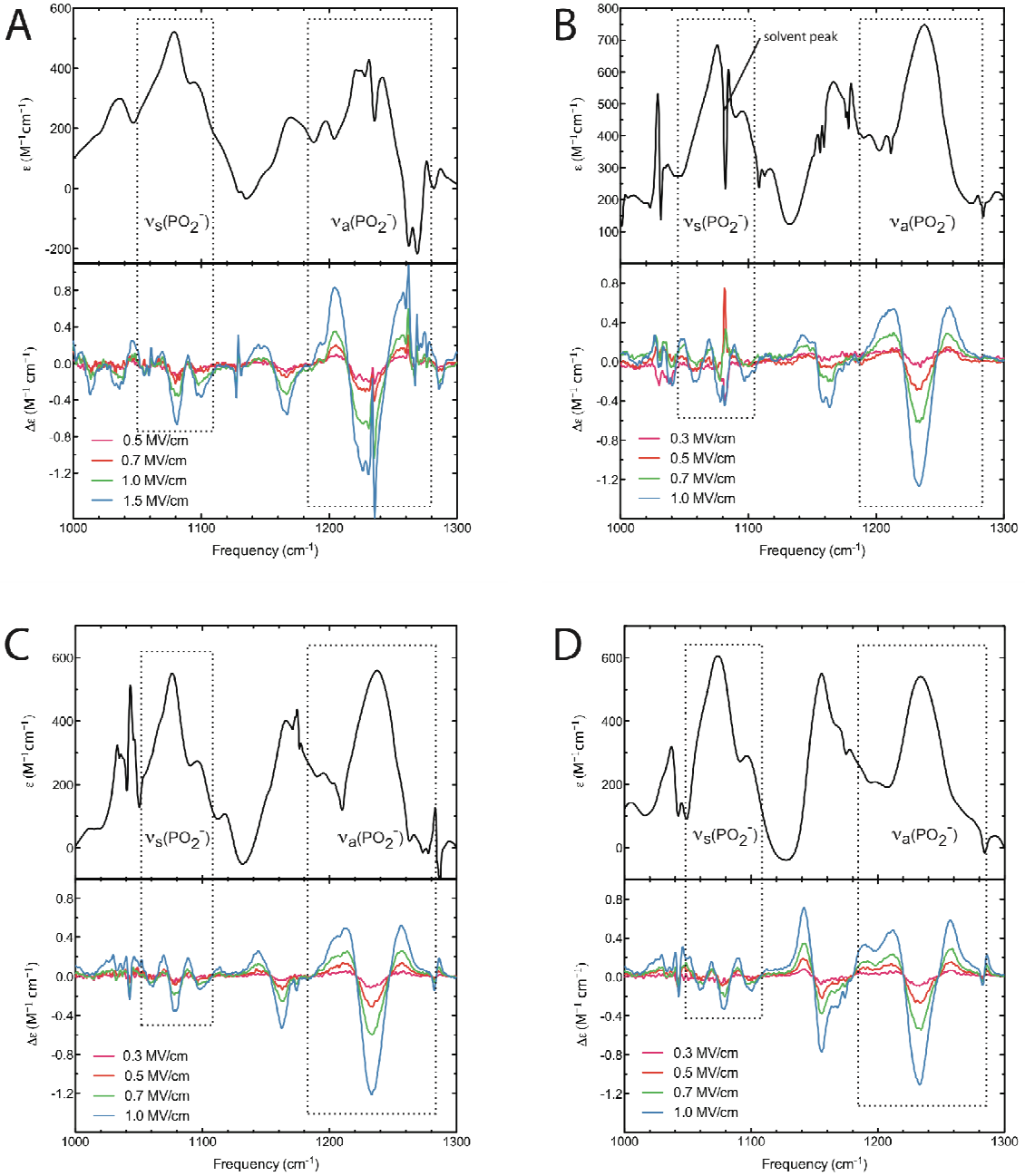

Figure S1. Absorbance (top panels) and Stark (bottom panels) spectra for all phospholipid/solvent samples. A) POPE in a 1:3 mixture of dichloromethane and dichloroethane. B) DOPE in toluene. C) DOPE in deuterated toluene. D) DDHEPE in deuterated toluene. The bands for the PO_2^- symmetric, $\nu_s(PO_2^-)$, and antisymmetric stretches, $\nu_a(PO_2^-)$, are indicated.

Hydration of phospholipid/toluene samples

All phospholipid/solvent samples exhibited similar red shifts of the PO_2^- antisymmetric stretch upon addition of stoichiometric amounts of water. The DDHEPE/toluene samples were hygroscopic, so in order to accurately measure the effect of hydration on the PO_2^- antisymmetric stretch frequency (Figure 2, main manuscript) we used DOPE/toluene samples, in which the degree of hydration could be more precisely controlled. In order to determine the effect of hydration on the Stark tuning rate of the PO_2^- antisymmetric stretch we used fresh DDHEPE/toluene samples to which either 2 or 4 molar equivalents of water were added. The absorbance and Stark spectra of these samples are shown in Figure S2 below. Note that the slight apparent decrease in the magnitude of the Stark effect for the hydrated samples can be attributed to a slight increase in the line width of the absorption bands, and the linear Stark tuning rates, extracted using the procedure described below, are the same, within error, for all three samples.

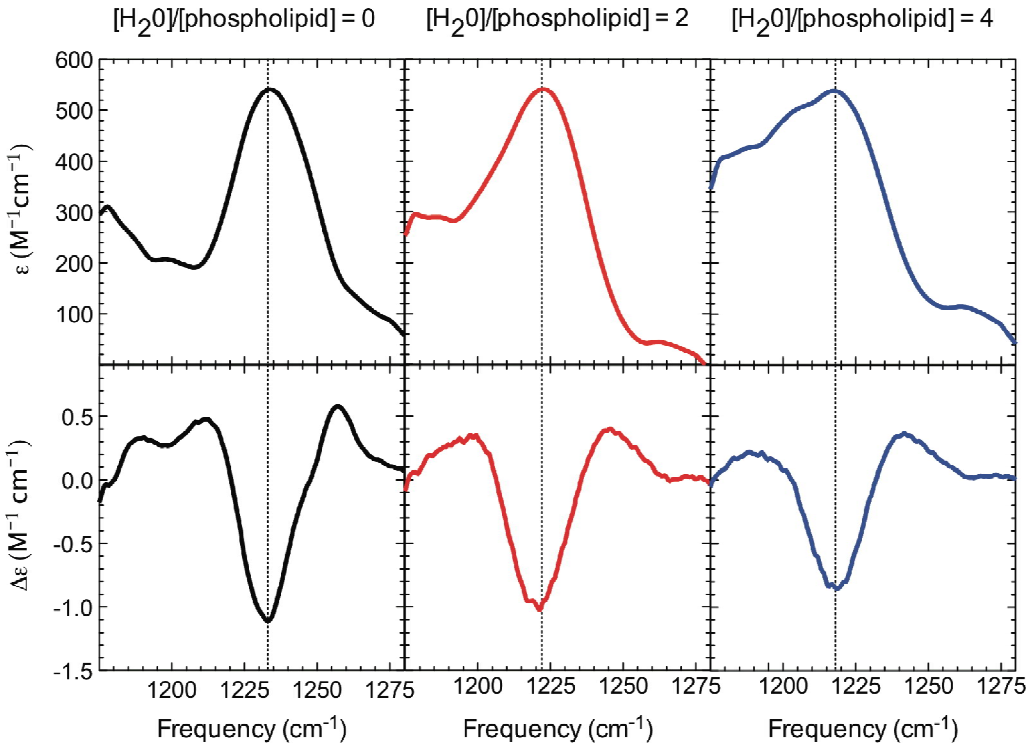

Figure S2. The antisymmetric stretch region of low temperature (77K) absorbance (top panels) and Stark (bottom panels) spectra are shown for DDHEPE/toluene samples to which either 0 (black), 2 (red) or 4 (blue) molar equivalents of water to phospholipid were added. The dotted lines indicate the peak centers.

Fitting the Stark spectra to determine the Stark parameters

Fitting of vibrational Stark spectra was performed as described previously[2]. For an isotropic sample the Stark spectrum can be expressed as a series of derivatives of the absorbance spectrum. The Stark spectra are fit to the derivatives of the absorbance and the Stark parameters of the sample are determined from the fitting coefficients. The magnitude of the linear Stark tuning rate, $|\Delta\vec{\mu}|$, is proportional to the square root of the

coefficient for the 2nd-derivative component of the Stark spectrum. In our absorption spectra the bands for the phosphate symmetric stretch were generally clear of overlapping features, allowing the Stark parameters to be determined by fitting the Stark spectra with derivatives of the experimental absorption spectra. In the case of the antisymmetric stretch derivatives of the absorption spectra were complicated by overlapping features, making such a fitting procedure unreliable. Instead, we determined the linear Stark tuning rate by fitting a Gaussian function to the absorbance spectrum and fitting the 2nd derivative of the Gaussian to the Stark spectrum. In this approach it is assumed that non-linear Stark effects are negligible, which is supported by the 2nd-derivative shape of the Stark spectrum for the antisymmetric stretch (Figure S1, lower panels). The linear Stark tuning rates we report here are based on the assumption that the angle ζ (the angle between the difference dipole and the transition dipole) was equal to 0 degrees for the symmetric stretch, and 90 degrees for the antisymmetric stretch. This is consistent with the results of our calculations (see the main manuscript).

Infrared absorbance spectrum of dimethyl phosphate in water

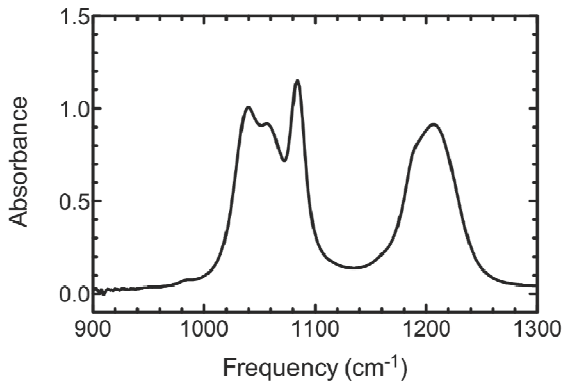

Figure S3. Absorbance spectrum of 1M dimethyl phosphate in water at pH 14.

Anharmonic Frequency Calculations

Anharmonic symmetric and antisymmetric stretch frequencies of the PO_2^- moiety of dimethyl phosphate (DMP, CH_3-O-PO_2-O-CH_3) were computed using a modified version of the methodology we have used in the past to compute anharmonic CD_2 vibrational frequencies[3-5]. First, the two-dimensional Born-Oppenheimer potential energy surface for the PO_2^- group was calculated using density functional theory (DFT) with the B3LYP[6-8] functional and a 6-311++G(d, p) basis set. Specifically, both PO bonds were stretched from 1.2 to 1.9 Å in 0.05 Å increments with the O-P-O angle, θ, held fixed. This produces a potential energy surface on a 15 × 15 grid (225 total single point energy calculations), where the coupling between the PO_2^- stretches and all other vibrations in the molecule are assumed to be negligible. The grid size and the distances over which the PO bonds were stretched were chosen by evaluating convergence of the symmetric and antisymmetric stretch PO_2^- frequencies for the isolated DMP molecule in its optimal geometry.

In our previous studies of CD_2 vibrations[3-5], we used far fewer grid points (typically an 8 × 8 grid with a spacing of 0.08 Å), and the vibrational frequencies were computed by fitting the potential energy to a model of two bilinearly coupled Morse oscillators. The eigenvalues for the resulting model were then computed by explicitly constructing its Hamiltonian in a basis of products of one-dimensional Morse oscillator wavefunctions and diagonalizing numerically. For the present application, in which accuracy is of paramount importance because the frequency shifts are exceedingly modest for applied electric fields in the range of ±0.0004 au, we chose to remove the intermediate step of fitting the potential energy data to a particular functional form. Greater accuracy could be achieved by instead utilizing a discrete variable representation (DVR) approach[9,10], which allows the vibrational eigenvalues to be obtained directly from the two-dimensional Born-Oppenheimer potential energy surface on a uniform grid. The two-dimensional Hamiltonian for the PO_2^- stretch vibrations is

$$H = \frac{p_x^2}{2\mu} + \frac{p_y^2}{2\mu} + \frac{p_x p_y \cos(\theta)}{m_{\mathrm{P}}} + V(x,y), \tag{1}$$

where x and y are the PO bond lengths, p_{x} and p_{y} are their conjugate momenta, μ is the reduced mass of the PO bond, θ is the O-P-O bond angle, and m_{P} is the mass of phosphorus. The coordinates, x and y, are then represented on a uniform grid with an odd number of points

$$\begin{aligned} x_j &= j\Delta x \qquad j = 0,\pm1,\pm2,...,\pm N \\ y_k &= k\Delta y \qquad k = 0,\pm1,\pm2,...,\pm N \end{aligned}, \tag{2}$$

where $\Delta x = \Delta y$ is the grid spacing. In a Fourier basis, the potential energy matrix is diagonal,

$$V_{jj',kk'} = \delta_{jj'}\delta_{kk'}V(x_j, y_k). \tag{3}$$

The complete Hamiltonian in the Fourier basis is,

$$H_{jj',kk'} = \delta_{kk'}T_{jj'} + \delta_{jj'}T_{kk'} + \frac{p_{jj'}p_{kk'}\cos(\theta)}{m_P} + \delta_{jj'}\delta_{kk'}V(x_j, y_k), \tag{4}$$

where $T_{jj'}$ and $p_{jj'}$ are discretized versions of the kinetic energy and momentum operators, respectively. Expressions for $T_{jj'}$ and $p_{jj'}$ in a Fourier basis have been obtained previously,[7,8] and are as follows,

$$T_{jj'} = \frac{\mathsf{h}^2(-1)^{j-j'}}{2\mu\Delta x^2}\begin{Bmatrix} \frac{\pi^2}{3} & j = j' \\ \frac{2}{(j-j')^2} & j \neq j' \end{Bmatrix}$$
$$p_{jj'} = \frac{\mathsf{h}(-1)^{j-j'}}{i\Delta x}\begin{Bmatrix} 0 & j = j' \\ \frac{1}{(j-j')} & j \neq j' \end{Bmatrix} \quad (5)$$

Using Equations (4) and (5) we then constructed the Hamiltonian matrix and diagonalized it numerically. The three lowest eigenvalues of the Hamiltonian, ε_0, ε_1, and ε_2 are sufficient to compute the symmetric and antisymmetric stretch PO_2^- transition frequencies of DMP,

$$\omega_s = \frac{\varepsilon_1 - \varepsilon_0}{\mathsf{h}}$$
$$\omega_a = \frac{\varepsilon_2 - \varepsilon_0}{\mathsf{h}} \quad . \quad (6)$$

Implicit Solvent Calculations

Implicit solvent calculations were performed on DMP to quantify the effects of solvent polarity on its symmetric and antisymmetric phosphate stretch frequencies. These calculations were performed in Gaussian 03 (full reference below) using the polarizable continuum model (PCM)[11]. In PCM calculations the solute of interest is embedded in a continuum with a specified dielectric constant. The cavity occupied by the solute is assumed to have a dielectric constant of unity and is constructed by centering spheres on each atomic cite with a radius corresponding to the van der Waals radius of the atom. The charge distribution of the solute polarizes the dielectric medium surrounding the cavity, which in turn polarizes the solute charge distribution. The electronic Schrödinger equation of the solute is solved using standard techniques (e.g. density functional theory), but with an additional iterative procedure to incorporate self-consistently the effects of solute-solvent polarization. It is important to note that only solute-solvent effects that are of electrostatic origin are captured by the PCM; other potentially important solute-solvent interactions, such as dispersion and repulsion, are not included in PCM calculations.

PCM calculations were performed for DMP for a range of solvent dielectric constants from $\varepsilon = 1.4$ (liquid argon) to $\varepsilon = 78.4$ (water). For each value of the solvent dielectric constant the geometry of the DMP was optimized using density functional theory (DFT) with the B3LYP[6-8] functional and a 6-311++G(d, p) basis set. A harmonic frequency analysis was then performed, from which the symmetric and antisymmetric phosphate

stretch frequencies were obtained. In Figure S4 the shifts in the DMP phosphate stretch frequencies relative to the gas phase are shown as a function of dielectric constant corresponding to 11 different solvents (argon, toluene, chlorobenzene, tetrahydrofuran, dichloroethane, acetone, ethanol, methanol, acetonitrile, dimethyl sulfoxide, and water). The antisymmetric phosphate stretch was shown to be considerably more sensitive to solvent polarity than the symmetric stretch. In water the PCM predicts a solvatochromic shift in the antisymmetric phosphate stretch frequency of -70.4 cm^{-1}, while the shift for the symmetric stretch is only -21.9 cm^{-1}. This result is consistent with the experimental finding that the vibrational Stark tuning rate of the phosphate antisymmetric stretch is considerably larger than that of the symmetric stretch. Interestingly, the implicit solvent calculations show a saturation in the solvatochromic shift for large values of the dielectric constant. For example, changing solvent from DMSO ($\varepsilon = 46.7$) to water ($\varepsilon = 78.4$) only results in a -1.7 cm^{-1} (-0.6 cm^{-1}) shift in the antisymmetric (symmetric) phosphate stretch frequency of DMP. A similar saturation in the phosphate antisymmetric stretch frequency is observed experimentally as the number of water molecules per phospholipid is increased in DOPE/toluene reverse micelles (Figure 2). For the phosphate antisymmetric stretch, the qualitatively similar behavior of the experimental results in Figure 2B and the implicit solvent calculations in Figure S4 suggest that the antisymmetric stretch is reporting on its local polarity. In contrast, for the symmetric stretch the discrepancy between the experimental blue-shift in response to hydration (Figure 2A) and the red-shift observed in the implicit solvent calculations suggests that the experimental blue-shifts are due to non-electrostatic quantum chemical effects that are not captured by the implicit solvent calculations.

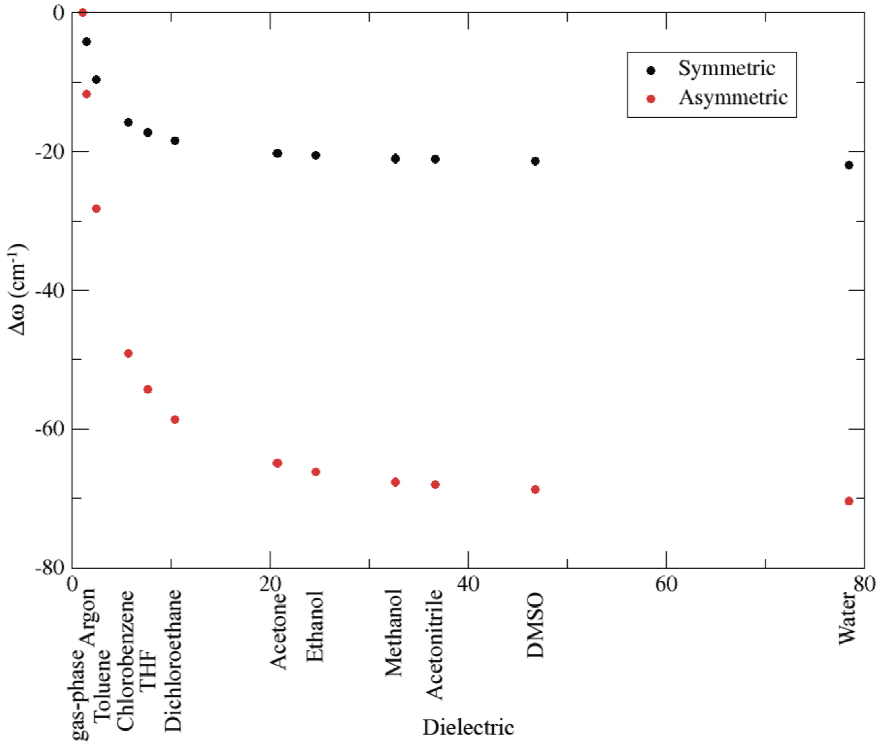

Figure S4. Calculated solvatochromic shift, relative to the gas-phase, in the symmetric and antisymmetric phosphate stretch frequencies of DMP in implicit solvents.

Complete Gaussian 03 Reference

Frisch, M. J.; Trucks, G. W.; Schlegel, H. B.; Scuseria, G. E.; Robb, M. A.; Cheeseman, J. R.; Montgomery Jr., J. A.; Vreven, T.; Kudin, K. N.; Burant, J. C.; Millam, J. M.; Iyengar, S. S.; Tomasi, J.; Barone, V.; Mennucci, B.; Cossi, M.; Scalmani, G.; Rega, N.; Petersson, G. A.; Nakatsuji, H.; Hada, M.; Ehara, M.; Toyota, K.; Fukuda, R.; Hasegawa, J.; Ishida, M.; Nakajima, T.; Honda, Y.; Kitao, O.; Nakai, H.; Klene, M.; Li, X.; Knox, J. E.; Hratchian, H. P.; Cross, J. B.; Bakken, V.; Adamo, C.; Jaramillo, J.; Gomperts, R.; Stratmann, R. E.; Yazyev, O.; Austin, A. J.; Cammi, R.; Pomelli, C.; Ochterski, J. W.; Ayala, P. Y.; Morokuma, K.; Voth, G. A.; Salvador, P.; Dannenberg, J. J.; Zakrzewski, V. G.; Dapprich, S.; Daniels, A. D.; Strain, M. C.; Farkas, O.; Malick, D. K.; Rabuck, A. D.; Raghavachari, K.; Foresman, J. B.; Ortiz, J. V.; Cui, Q.; Baboul, A. G.; Clifford, S.; Cioslowski, J.; Stefanov, B. B.; Liu, G.; Liashenko, A.; Piskorz, P.; Komaromi, I.; Martin, R. L.; Fox, D. J.; Keith, T.; Al-Laham, M. A.; Peng, C. Y.; Nanayakkara, A.; Challacombe, M.; Gill, P. M. W.; Johnson, B.; Chen, W.; Wong, M. W.; Gonzalez, C.; Pople, J. A.; *Gaussian 03 Revision C.02;* Gaussian Inc.: Wallingford, CT, 2004.

References

(1) Chia, N. C.; Mendelsohn, R. *J Phys Chem-Us* **1992**, *96*, 10543.
(2) Andrews, S. a. B., SG *J. Phys. Chem. A* **2000**, *104*, 11853.
(3) Miller, C. S.; Corcelli, S. A. *J. Phys. Chem. B* **2009**, *113*, 8218.
(4) Miller, C. S.; Corcelli, S. A. *J. Phys. Chem. B* **2010**, *114*, 8565.
(5) Miller, C. S.; Ploetz, E. A.; Cremeens, M. E.; Corcelli, S. A. *J. Chem. Phys.* **2009**, *130*, 125103.
(6) Becke, A. D. *J. Chem. Phys.* **1993**, *98*, 5648.
(7) Lee, C. T.; Yang, W. T.; Parr, R. G. *Phys. Rev. B* **1988**, *37*, 785.
(8) Miehlich, B.; Savin, A.; Stoll, H.; Preuss, H. *Chem. Phys. Lett.* **1989**, *157*, 200.
(9) Colbert, D. T.; Miller, W. H. *J. Chem. Phys.* **1992**, *96*, 1982.
(10) Seideman, T.; Miller, W. H. *J. Chem. Phys.* **1992**, *97*, 2499.
(11) Tomasi, J.; Mennucci, B.; Cammi, R. *Chem. Rev.* **2005**, *105*, 2999.